Localization and Band Gap Pinning in Semiconductor Superlattices with Layer Thickness Fluctuations

1995 Europhys. Lett. 31 107

(http://iopscience.iop.org/0295-5075/31/2/008)

EUROPHYSICS LETTERS 10 July 1995

Europhys. Lett., **31** (2), pp. 107-112 (1995)

Localization and Band Gap Pinning in Semiconductor Superlattices with Layer Thickness Fluctuations.

K. A. MÄDER (*) and A. ZUNGER

National Renewable Energy Laboratory - Golden, CO 80401, USA

(received 1 November 1994; accepted in final form 16 June 1995)

PACS. 73.20Dx – Electron states in low-dimensional structures (including quantum wells, superlattices, layers structures, and intercalation compounds).

PACS. 71.50+t – Localization single-particle electronic states (excluding impurities).

Abstract. – We consider $(AlAs)_n/(GaAs)_n$ superlattices with random thickness fluctuations Δn around the nominal period n. Using three-dimensional pseudopotential plane-wave band theory, we show that i) *any* amount $\Delta n/n$ of thickness fluctuations leads to band edge wave function localization, ii) for small $\Delta n/n$ the SL band gap is pinned at the gap level produced by a *single* layer with «wrong» thickness $n + \Delta n$, iii) the bound states due to monolayer thickness fluctuations lead to significant band gap reductions, *e.g.*, in $n = 2$, 4, 6, and 10 monolayer SLs the reductions are 166, 67, 29, and 14 meV for $\langle 111 \rangle$ SLs, and 133, 64, 36, and 27 meV for $\langle 001 \rangle$ SLs, iv) $\langle 001 \rangle$ AlAs/GaAs SLs with monolayer thickness fluctuations have a direct band gap, while the ideal $\langle 001 \rangle$ SLs are indirect for $n < 4$.

The electronic structure and quantum confinement effects in semiconductor superlattices are usually modeled by assuming an *ideal* structure, *i.e.*, that the interfaces are atomically abrupt and that the individual layer thicknesses remain constant throughout the superlattice [1, 2]. Actual heterostructures, however, often deviate from ideality in two ways: i) *lateral* imperfections in the (x, y)-plane, such as intermixed [3], stepped [4], or islanded [5] interfaces, and ii) *vertical* (z-direction), discrete thickness fluctuations around its nominal value, even though the interfaces could remain reasonably flat and atomically abrupt in the (x, y)-plane [6]. It is likely that both types of interfacial imperfections coexist in many samples [7]. In case i) the translational symmetry is broken *in the substrate plane* (x, y), and the concentration profile along the growth direction is continuous («graded» or «intermixed» interfaces), while in case ii) a discrete, rectangular-shaped concentration profile exists, but the superlattice translational symmetry is broken *along the growth direction* z. Case i) has been modeled theoretically by assuming graded (rather than square) potential wells [8], or by considering supercells with atomic swaps across the interfaces [9]. In this paper we consider layer-thickness fluctuations (case ii)), *i.e.*, $(A)_n/(G)_n$ superlattices (SLs) with nominal layer thicknesses of n monolayers (MLs) of material A = AlAs and n ML of material G = GaAs, but where each layer is occasionally thinner or thicker than its intended thickness n. We use a three-dimensional pseudopotential band structure description within a highly flexible plane-wave basis [10], rather than one-dimensional effective-mass models [11], or one-dimensional [12] or three-dimensional [13] tight-binding models.

Superlattices with layer thickness fluctuations are described by supercells containing

(*) Present address: CECAM, Ecole Normale Supérieure, 46, Allée d'Italie, 69364 Lyon cedex 07, France. E-mail: mader@cecam.fr.

several hundreds of atoms [14]. The novel empirical pseudopotentials used here [10] have been tested extensively for AlAs/GaAs bulk materials, short-period superlattices, and random alloys. The results [10] compare well with experiment and with state-of-the-art, self-consistent pseudopotential calculations, however, without suffering from the band gap underestimation of the local-density approximation [10]. For periods $n \leqslant 20$ we consider *single monolayer fluctuations*, so the layer thicknesses are in the set $\{n-1, n, n+1\}$, while for $n > 20$ we consider a fixed fraction $\Delta n/n$ of layer thickness fluctuations Δn.

We find that: i) *any* amount $\Delta n/n$ of thickness fluctuations leads to band edge wave function localization, ii) for small $\Delta n/n$ the SL band gap is pinned at the gap level produced by a *single* layer with «wrong»thickness $n' \neq n$ (a «chain mutation»), iii) the bound states due to monolayer thickness fluctuations lead to band gap reductions that monotonically decrease with increasing n. These fluctuation-induced bound states will photoluminesce at energies below the «intrinsic» absorption edge. iv) $\langle 001 \rangle$ AlAs/GaAs SLs with monolayer thickness fluctuations have a direct band gap, while the ideal $\langle 001 \rangle$ SLs are indirect for $n < 4$.

Consider first, by way of reference, the band structure of *ideal* AlAs/GaAs SLs with layers oriented along (111) or (001) (fig. 1). In agreement with previous theoretical studies [2], we find that i) the ideal $\langle 111 \rangle$ SL has a *direct* band gap for all n values, since the conduction band minimum (CBM) is the Γ-folded $\bar{\Gamma}_{1c}(\Gamma_{1c})$ state. This SL has a «type-I» band arrangement with both the highest valence and the lowest conduction state localized on the GaAs layers. ii) The second conduction band at $\bar{\Gamma}$ is folded from the zincblende Γ-L_z bands; for small n the pseudodirect $\bar{\Gamma}_{1c}(L_{1c})$ state mixes strongly with the direct $\bar{\Gamma}_{1c}(\Gamma_{1c})$ state. The mixing, and thus the level repulsion, shows odd-even oscillations for small n (reflecting localization of repelling states on the same or on either sublattice [2]). Note that the

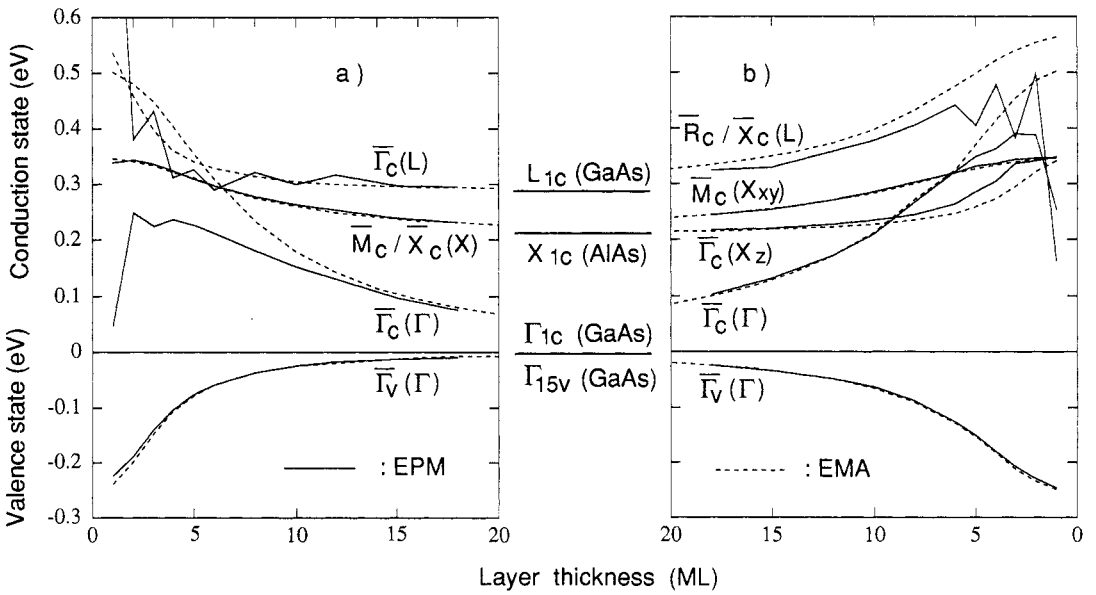

Fig. 1. – Energy levels of *ideal* $(AlAs)_n/(GaAs)_n$ superlattices along *a*) $\langle 111 \rangle$ and *b*) $\langle 001 \rangle$, as a function of period n. The bulk levels in the middle column are reached asymptotically as $n \to \infty$. Γ_{15v}(AlAs) is 500 meV below the GaAs VBM. The SL states are denoted with an overbar, while their parent zincblende states Γ, X, and L are given in parentheses. The dashed lines are obtained from a one-band envelope function model using the effective masses and band offset from our pseudopotential calculation [15].

one-dimensional effective-mass model (dashed lines [15] in fig. 1) completely misses the strong non-monotonic variations of SL energy levels with layer thickness.

The situation is very different for ⟨001⟩-oriented ideal SLs. The prominent properties apparent in fig. 1*b*) are: i) the $n = 1$ SL has an *indirect* band gap at the L-folded point $\overline{R}$ [1,2]; ii) for $n < 4$, the lateral $X_{x,y}$ valleys (folded to $\overline{M}$) and the X_z valley (folded to $\overline{\Gamma}$) are nearly degenerate [16]; iii) for $1 < n \leqslant 8$ the pseudodirect, AlAs-like $\overline{\Gamma}_{1c}(X_z)$ state is below the direct, GaAs-like $\overline{\Gamma}_{1c}(\Gamma_{1c})$ state, thus the SL is type II; for $n > 8$, however, $\overline{\Gamma}_{1c}(\Gamma_{1c})$ is lower, so the system is type I (experimentally, the type-II/type-I crossover is found at $n \approx 11$ [16]);

We now allow the layer thicknesses in the $n \times n$ SLs to fluctuate around the ideal value n by ± 1 ML. The growth sequence is now defined in terms of a *distribution function* $p(n')$, which we assume to be uncorrelated and symmetric around the nominal thickness n. We define the relative frequency R of monolayer fluctuations by

$$p(n \pm 1) = R\,p(n)\,. \tag{1}$$

Because the distribution $p(n')$ is normalized, we can write $p(n) = 1/(1 + 2R)$ and $p(n \pm 1) = R/(1 + 2R)$. For the *ideal* $n \times n$ superlattice $R = 0$, and $p(n') = \delta(n' - n)$, whereas for $R = 1$ the layer thicknesses $\{n - 1, n, n + 1\}$ occur with equal probability $p = 1/3$. A single chain mutation in a finite superlattice of length N monolayers corresponds to $R \approx (2n/N)$, which will be denoted here as the $R \to 0$ limit (to be distinguished from $R = 0$ with no mutations). To simulate the lack of periodicity along the growth direction, we have used supercells of a total length N between 100 and 1000 ML, and repeated these supercells periodically. A particular growth sequence was created by a random number generator, specifying n, N and R.

The band edge energies of $(AlAs)_n/(GaAs)_n$ SLs with *one-monolayer thickness fluctuations* about n are plotted in fig. 2 relative to the band edges of the *ideal* SLs (the energy zero). We see that: i) thickness fluctuations create both hole ($\Delta\varepsilon_h$) and electron ($\Delta\varepsilon_e$) bound states for *any degree* of thickness fluctuation ($0 < R \leqslant 1$), ii) the band gap reductions $\Delta E_g = \Delta\varepsilon_h + \Delta\varepsilon_e$ decay with n, and have a definite dependence on superlattice direction; they

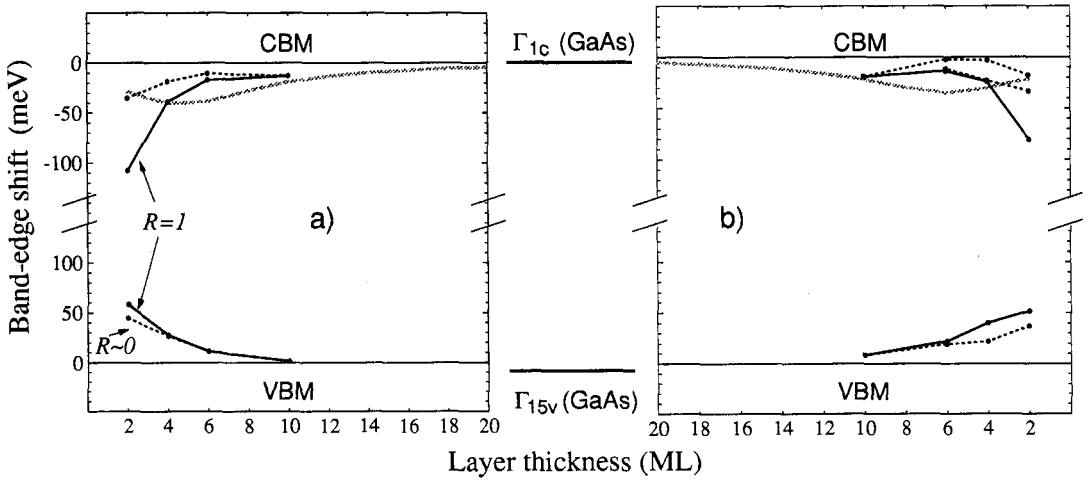

Fig. 2. – Gap levels in the presence of one-monolayer thickness fluctuations in $(AlAs)_n/(GaAs)_n$ superlattices along *a*) ⟨111⟩ and *b*) ⟨001⟩, as a function of period n. Energies are measured with respect to the band extrema of the *ideal* $n \times n$ SL (see fig. 1). One-band envelope function results for a $(n + 1)$-ML mutation embedded in the $n \times n$ SL are indicated by a dashed gray line. $R = 1$ and $R \to 0$ denote, respectively, the concentrated and dilute limit of chain mutations (eq. (1)).

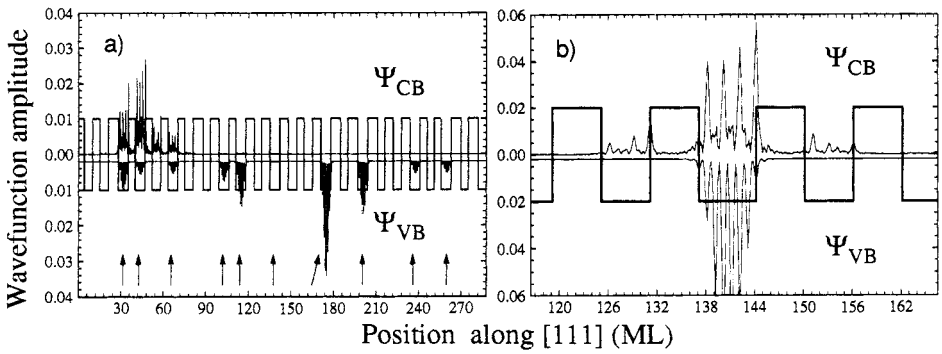

Fig. 3. – Planar averages of wave functions squared of the CBM and VBM in the $(AlAs)_6/(GaAs)_6$ SL along $\langle 111 \rangle$ with ± 1 layer thickness fluctuations. Hole wave functions are plotted in the negative direction, with a small offset for clarity. *a*) Concentrated limit ($R = 1$), *b*) dilute limit ($R \to 0$), *i.e.*, a single $(GaAs)_7$ mutation embedded in a 6×6 SL host. The rectangular-shaped lines show the growth sequence of the SL, with GaAs layers represented by wells, and AlAs layers represented by barriers, respectively. The vertical arrows in *a*) indicate the 7 ML thick, «mutated» wells.

are 166, 67, 29, and 14 meV for $n = 2, 4, 6$, and 10 in the $\langle 111 \rangle$ direction, and 133, 64, 36, and 27 meV in the $\langle 001 \rangle$ direction, respectively, iii) the dilute limit of a single chain mutation already produces a *finite gap reduction* $\Delta E_g(R \to 0)$, iv) $\Delta E_g(R \to 0)$ merges with $\Delta E_g(R = 1)$ at $n \gtrsim 6$, at which point the gap reduction becomes independent («band gap pinning») of the number of chain mutations.

The appearance of gap levels in SLs with one-monolayer thickness fluctuations is accompanied by *wave function localization*. For example, inspection of the CBM wave function of an $n = 6$ $\langle 111 \rangle$ superlattice with random ± 1 monolayer fluctuations (fig. 3*a*)) reveals that it is localized on ~ 4 GaAs wells, with minimal amplitude in the AlAs barriers and maximal amplitude on the two neighboring mutated (7-ML) GaAs wells («twin» fluctuation denoted by bold arrows). The CBM thus resembles a bound state in a coupled double quantum well. The hole wave function at the valence band maximum (VBM) is likewise localized on a number of mutated, 7-ML GaAs wells (fig. 3*a*)); in contrast to the CBM, however, the reason for the multi-well pattern of the VBM wave function is that these states are in fact decoupled, quantum-well–confined states, which are degenerate in energy within the accuracy of our calculation ($\lesssim 0.1$ meV). A typical hole and electron wave function localized on an *isolated* $(GaAs)_7$ mutation in an otherwise ideal 6×6 $\langle 111 \rangle$ SL are shown in fig. 3*b*). We see that the hole wave function of an isolated mutation ($R \to 0$) resembles that of the concentrated ($R = 1$) mutations (fig. 3*a*)), and its binding energy $\Delta\varepsilon_h(R \to 0) = 11$ meV equals the value at $R = 1$. At the CBM, the larger penetration of the wave function into neighboring GaAs wells can produce deeper gap states, and consequently pinning occurs at a larger n ($n_p \approx 10$) than for hole states.

Experimentally, the fluctuation-induced localized bound states should be observable as photoluminescence centers whose energy is below the absorption edge of the underlying «ideal» SL structure. This photoluminescence will lack phonon lines, because the optical transitions are direct in the planar Brillouin zone (the transverse wave vector $\boldsymbol{k}_\perp$ is still a good quantum number), and because the k_z selection rule is relaxed by vertical disorder. Indeed, while calculations [2] on *ideal* $\langle 111 \rangle$ $(AlAs)_n/(GaAs)_n$ SLs predicted a direct band gap with a type-I band arrangement, Cingolani *et al.* [17] noted a ~ 100 meV red shift of the photoluminescence at 1.80 eV relative to the absorption in $(AlAs)_6/(GaAs)_6$ $\langle 111 \rangle$ SLs, interpreting this as reflecting a type-II band arrangement. However, since they noted that their

SL had a ± 1 ML period uncertainty, it is possible that the red-shifted photoluminescence originates from thickness fluctuation bound states. Our calculated band gap of the $n = 6$ superlattice with ± 1 ML thickness fluctuations is 1.78 eV for $R = 1$, and 1.80 eV for $R \to 0$, close to their observed photoluminescence peak position (1.80 eV) [17] [1].

Figure 2 shows that the bound states of *isolated* mutations ($R \to 0$) merge with those of concentrated layer thickness fluctuations ($R \to 1$) at some «pinning period» n_p. In what follows we discuss the i) $n < n_p$ and ii) $n \geq n_p$ regimes. In the short-period regime ($n < n_p$), the band gap reduction depends on R. This regime coincides with the region in fig. 1 where the band gaps of the *ideal* SLs have a complex n-dependence, showing strong non-effective-mass behavior. The $\langle 001 \rangle$ $(AlAs)_2/(GaAs)_2$ SL with monolayer fluctuations is in fact identical to the *intentionally disordered* SL grown by Sasaki *et al.* [18]. In that structure, A_2 and G_2 layers are randomly replaced by A_1, A_3, G_1, and G_3 layers. We find the following changes in the band structure when the layer thicknesses fluctuate by ± 1 ML: i) For the $n = 2$ $\langle 001 \rangle$ SL we obtain $\Delta\varepsilon_e(R = 1) = 22$, 81, and 171 meV at $\bar{M}$, $\bar{\Gamma}$, and $\bar{X}$ in the planar Brillouin zone. Since the level shift $\Delta\varepsilon_e$ at $\bar{\Gamma}$ exceeds the one at $\bar{M}$ by ~ 60 meV, layer thickness fluctuations transform the indirect 2×2, ideal superlattice into a direct-gap material [19]. The large binding energy at $\bar{X}$ originates from the increased level repulsion of the folded L_{1c} states when the translational and rotational symmetry of the ideal $n = 2$ superlattice is broken. This level repulsion is larger for odd n than for even n, and it leads to an L-like, indirect CBM for $n = 1$ (fig. 1*b*)). ii) The $n = 2$ $\langle 001 \rangle$ SL is direct even in the $R \to 0$ limit of isolated chain mutations. iii) Numerous electron and hole states are localized on the same spatial region along z, hence the $\langle 001 \rangle$ SLs with thickness fluctuations will exhibit type-I, rather than type-II characteristics as ideal $n < 10$ SLs do. iv) While for $n > n_p$ only mutated, wider GaAs wells bind a carrier (see below), in the short-period $\langle 001 \rangle$ case even an $(AlAs)_{n+1}$ mutation binds an electron. In fact, the AlAs-like bound electron lies *deeper* in the gap than the GaAs-like bound electron (see the two dotted lines near the CBM in fig. 2*b*)).

We next discuss the SL properties in the regime of band gap pinning $n \geq n_p$. At this point the band gap reduction is pinned at the value

$$\Delta E_g(R) = \lim_{R \to 0} \Delta E_g(R) = \Delta\varepsilon_e + \Delta\varepsilon_h \,, \tag{2}$$

where $\Delta\varepsilon_e$ ($\Delta\varepsilon_h$) is the electron (hole) binding energy of an *isolated* ($R \to 0$) layer mutation. Qualitatively, eq. (2) can be understood in terms of a one-dimensional effective-mass picture, where the SL is modeled by a Kronig-Penney model, with the usual boundary conditions of a continuous envelope function $F(z)$ and current $(1/m^*)F'(z)$, where the effective mass m^* is different in the well and barrier material. Each of the $(n + 1)$-ML mutations gives rise to a bound state below the band edge of the $n \times n$ SL [11, 20]. The gray lines in fig. 2 indicate that this simple picture is expected to agree *quantitatively* with our pseudopotential calculation for $n \geq 10$ (note, however, the large discrepancy with our three-dimensional calculation at smaller n's). For very large n, when the quantum wells are completely decoupled, the SL energy spectrum is simply that of degenerate single quantum wells. Hence the extra binding energy of an $(n + \Delta n)$-ML mutation approaches asymptotically

$$\Delta\varepsilon_c = \varepsilon_0(n) - \varepsilon_0(n + \Delta n) \approx \frac{2\,\Delta n}{n}\,\varepsilon_0(n) \,, \tag{3}$$

---

[1] We have separately studied the influence of atomic intermixing within 2 ML across the interface, and found that the direct band gap is blue-shifted from 1.81 eV in the ideal SL to ~ 1.89 eV, close to the observed [17] absorption edge (1.90 eV). However, we have not studied the *combined* influence of ML fluctuations and intermixing on the band gaps, and can only speculate that the experimental results might be compatible with the coexistence of these two types of imperfections.

where $\varepsilon_0(n)$ is the ground-state energy of a carrier with mass m^* in a n-ML wide quantum well, which scales like $1/m^* n^2$ for large n. Using a fixed $\Delta n/n = 10\%$, we obtain from the first equality of eq. (3) $\Delta\varepsilon_e = 10.0$, 2.4 and 0.7 meV for $n = 20$, 50 and 100 in the $\langle 111 \rangle$ SL (the last equality of eq. (3) gives 14.3, 3.0 and 0.8 meV, respectively). The band gap reduction for a given $\Delta n/n$ is obtained by inserting $\Delta\varepsilon_h$ and $\Delta\varepsilon_e$ from eq. (3) in eq. (2). The degeneracy of the gap level $\Delta\varepsilon_c$ is equal to the number $M_{n+\Delta n}$ of $(n + \Delta n)$-ML well mutations, which, in the case of $\Delta n = 1$ (see eq. (1)), is given by

$$M_{n+1} \approx \frac{R}{1+2R} \frac{N}{2n} . \tag{4}$$

Using eqs. (3) and (4) one can predict the band gap reduction and number of localized states in the multiple quantum well regime.

In summary, we have shown that discrete layer thickness fluctuations in $(AlAs)_n/(GaAs)_n$ superlattices lead to i) localization of the wave functions near the band edges, ii) a reduced band gap, which is pinned at the value corresponding to an isolated layer thickness fluctuation for $n > n_p$, and iii) a crossover to a direct band gap in the case of short-period $\langle 001 \rangle$ SLs.

* * *

We wish to thank L.-W. WANG for discussions and for performing the envelope function model calculations of fig. 1 and 2. This work was supported by the Office of Energy Research, Materials Science Division, U.S. Department of Energy, under grant No. DE-AC36-83CH10093.

REFERENCES

[1] BYLANDER D. M. and KLEINMAN L., *Phys. Rev. B*, **34** (1986) 5280.
[2] WEI S.-H. and ZUNGER A., *Appl. Phys. Lett.*, **53** (1988) 2077; IKONIĆ Z., SRIVASTAVA G. P. and INKSON J. C., *Phys. Rev. B*, **46** (1992) 15150.
[3] OURMAZD A. *et al.*, *Phys. Rev. Lett.*, **62** (1989) 933; GRANT J. *et al.*, *Appl. Phys. Lett.*, **59** (1991) 2859.
[4] FEENSTRA R. M. *et al.*, *J. Vac. Sci. Technol. B*, **12** (1994) 2592.
[5] BIMBERG D. *et al.*, *J. Vac. Sci. Technol. B*, **5** (1987) 1191.
[6] FUJIWARA K. *et al.*, *Appl. Phys. Lett.*, **51** (1987) 1717; KOPF R. F. *et al.*, *Appl. Phys. Lett.*, **58** (1991) 631; PARKS C. *et al.*, *Phys. Rev. B*, **48** (1993) 5413.
[7] WARWICK C. A. *et al.*, *Appl. Phys. Lett.*, **56** (1990) 2666; BELITSKY V. I. *et al.*, *Phys. Rev. B*, **49** (1994) 8263.
[8] NELSON D. F. *et al.*, *Phys. Rev. B*, **36** (1987) 8063.
[9] LAKS D. B. and ZUNGER A., *Phys. Rev. B*, **45** (1992) 11411; JAROS M. AND BEAVIS A. W., *Appl. Phys. Lett.*, **63** (1993) 669.
[10] MÄDER K. A. and ZUNGER A., *Phys. Rev. B*, **50** (1994) 17393.
[11] LITTLETON R. K. and CAMELY R. E., *J. Appl. Phys.*, **59** (1986) 2817; IHM G. *et al.*, *Phys. Rev. B*, **46** (1992) 9564.
[12] DOW J. D., REN S. Y. and HESS K., *Phys. Rev. B*, **25** (1982) 6218; STROZIER J. *et al.*, *J. Vac. Sci. Technol. A*, **11** (1993) 923.
[13] WANG E. G., SU W. P. and TING C. S., *J. Appl. Phys.*, **76** (1994) 3004.
[14] WANG L.-W. and ZUNGER A., *J. Chem. Phys.*, **100** (1994) 2394.
[15] WANG L.-W., private communication (1995).
[16] GE W. *et al.*, *J. Lumin.*, **59** (1994) 163.
[17] CINGOLANI R., TAPFER L. and PLOOG K., *Appl. Phys. Lett.*, **56** (1990) 1233.
[18] SASAKI A. *et al.*, *Jpn. J. Appl. Phys.*, **28** (1989) L1249; *J. Crystal Growth*, **115** (1991) 490.
[19] MÄDER K. A., WANG L.-W. AND ZUNGER A., *Phys. Rev. Lett.*, **74** (1995) 2555.
[20] CHOMETTE A. *et al.*, *Phys. Rev. Lett.*, **57** (1986) 1464; PAVESI L. *et al.*, *Phys. Rev. B*, **39** (1989) 7788.